

Segmented Polyurethane Elastomers with Liquid Crystalline Hard Segments. 1. Synthesis and Phase Behavior

Weiming Tang, Richard J. Farris, and William J. MacKnight*

Department of Polymer Science and Engineering, University of Massachusetts, Amherst, Massachusetts 01003

Claus D. Eisenbach

Makromolekulare Chemie II, Universität Bayreuth, 95440 Bayreuth, Federal Republic of Germany

Received October 17, 1993; Revised Manuscript Received January 24, 1994*

ABSTRACT: Segmented liquid crystalline polyurethanes (LCPUE) have been studied with hard segments composed of the mesogen 4,4'-bis(6-hydroxyhexoxy)biphenyl, 2,4-tolylene diisocyanate, and 2,6-tolylene diisocyanate and soft segments composed of poly(tetramethylene oxides). Differential scanning calorimetry and wide-angle X-ray scattering experiments show the existence of an enantiotropic mesophase in the hard domains of the elastomer. Compared with nonsegmented polyurethane containing the same mesogen, the isotropization temperature of the mesophase in the elastomer is depressed. This is a result of the oligomeric structure of the hard domains. The endotherm corresponding to the isotropization transition is also broadened, reflecting a lack of uniformity of the hard domains. Furthermore, the mesophase can be oriented by elastic deformation, and it forms a more ordered structure during this process. The tensile properties of these segmented polyurethanes are determined by their morphologies and can be manipulated by controlling the hard- and soft-segment concentration ratio.

Introduction

Segmented block copolymers with alternating sequences of hard and soft segments are an important class of thermoplastic elastomers. The thermodynamic incompatibility between the hard and soft segments normally results in a microphase-separated structure. The hard segments form glassy or crystalline domains which act as physical cross-links to form a network. For example, in polyurethane elastomers, the hard segments based on diphenylmethane-4,4'-diisocyanate and short-chain diols develop crystallinity in the hard domains which act as multifunctional junction points and fillers.

Elastomeric chemically cross-linked networks with liquid crystalline side chains have been described,^{1,2} and a few studies in the literature report the introduction of mesogens into the hard segment in the physically cross-linked thermoplastic elastomers.^{3,4} The resulting polymeric structure consists of alternating liquid crystalline and amorphous segments which form main-chain liquid crystalline elastomers, a new class of polymeric material. The elasticity of this novel material arises from the conformational entropy changes which the soft segments undergo upon stretching, and the mesophase can be oriented by mechanical strain. Due to the liquid crystalline nature of the hard domains, their response to an applied strain should be different than that in a system with crystalline domains, and such an applied strain may result in a highly oriented and perfected structure. At high elongations, the amorphous soft segments will tend to become anisotropic as well. Thus, this kind of elastomer may exhibit unusual anisotropic mechanical, electrical, and optical properties, leading to future technological applications.

Thermotropic liquid crystalline polyurethanes have been studied⁵⁻⁹ for their potential application as high-strength fibers and plastics. In our previous studies, both the isomerically pure 2,4-tolylene diisocyanate- and 2,6-

tolylene diisocyanate-4,4'-bis(6-hydroxyhexoxy)biphenyl polyurethanes were found to be crystallizable and also to display monotropic liquid crystalline phases. Cocrystallization of the isomerically pure polymers does not occur. The crystalline phase can be destabilized relative to the liquid crystalline phase, thus forming an enantiotropic liquid crystalline phase by altering the structure of the polymer, for example, by copolymerization and/or blending of the isomers. Stenhouse and MacKnight¹⁰ obtained an enantiotropic liquid crystalline polyurethane (referred to as LCPU) from 4,4'-bis(6-hydroxyhexoxy)biphenyl with 2,4-tolylene diisocyanate and 2,6-tolylene diisocyanate at equal molar ratio. The current elastomers (referred to as LCPUE) are based on this LCPU structure as the hard segment, and we have compared the properties of LCPUE with LCPU in view of the understanding of the behavior of the mesophase in the elastomers. Poly(tetramethylene oxide) with different molar masses (650, 1000, 2000) is used as the soft segment.

Experimental Section

Materials. 2,4-Tolylene diisocyanate (2,4-TDI; Fluka) and 2,6-tolylene diisocyanate (2,6-TDI; Aldrich) were purified by vacuum distillation. Poly(tetramethylene oxides) (PTMO; M_w = 650, 1000, 2000; PolyScience) were dried in vacuo for 3 days at 50 °C. Dimethylformamide (DMF) was dried over molecular sieves and distilled under reduced pressure. 6-Chloro-1-hexanol (97%), 4,4'-dihydroxybiphenyl, ethyl alcohol, and 1,4-dioxane were used as received.

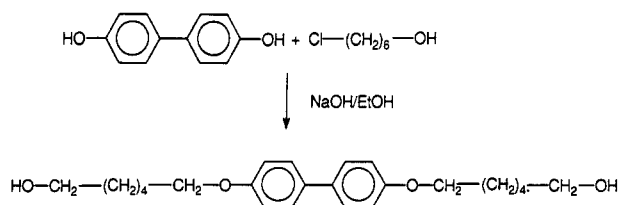
The syntheses of the mesogenic chain extender 4,4'-bis(6-hydroxyhexoxy)biphenyl (Diol-6) and of liquid crystalline polyurethane elastomers (LCPUE) are outlined in Schemes 1 and 2.

4,4'-Bis(6-hydroxyhexoxy)biphenyl (Diol-6).⁵ A total of 90 mL of ethyl alcohol was placed in a 250-mL three-necked flask equipped with a dropping funnel, a reflux condenser, and a magnetic stirrer. To this flask were added NaOH (6.72 g, 0.168 mol) and 4,4'-dihydroxybiphenyl (7.7 g, 0.042 mol), and the mixture was heated to 70 °C. 6-Chloro-1-hexanol (25 g, 0.183 mol) was added dropwise. The reaction mixture was refluxed for 24 h and poured into water. The precipitated material was filtered off and recrystallized three times from dioxane to yield

* To whom correspondence should be addressed.

* Abstract published in *Advance ACS Abstracts*, April 1, 1994.

Scheme 1



a white powdery compound. Mp: 174.0–174.5 °C. ^1H NMR (DMF- d_7): δ 1.33–1.79 (m, 16 H, $-(\text{CH}_2)_4-$), 3.51 (t, 4 H, CH_2OH), 4.02 (t, 4 H, $-\text{CH}_2\text{OAr}$), 4.36 (t, 2 H, OH), 7.02 (d, 4 H, *o*-phenoxy), 7.56 (d, 4 H, *m*-phenoxy).

Synthesis of Liquid Crystalline Polyurethane Elastomers (LCPUE). Conventional polyurethane synthesis conditions were used for the preparation of LCPUE.^{11–13}

To a 500-mL four-necked flask equipped with a condenser, thermometer, mechanical stirrer, and argon inlet-outlet were successively added PTMO ($M_w = 650, 1000, 2000$) (0.007 83 mol), the 1:1 (w/w) mixture of 2,4-tolylene diisocyanate (1.36 g, 0.007 83 mol), and 2,6-tolylene diisocyanate (1.36 g, 0.007 83 mol). The reaction mixture was mechanically stirred at 100 °C under argon for 2.5 h. Then DMF (15 mL) and Diol-6 (3.02 g, 0.007 82 mol) were added, and the reaction was held at 100 °C for 50 h. DMF was added as the reaction proceeded to keep the solution viscosity low enough to allow stirring. The white polymer was precipitated out by pouring the hot, solution into methanol. After Soxhlet extraction of material in methanol to remove DMF and unreacted starting material, the product was dried in vacuo.

The list of the chemical shifts of the ^{13}C NMR spectrum in LCPUE is given in Table 1. The spectrum was obtained with a 20-s recycle delay and the decoupler gated off except during acquisition.

Polymer Characterization Techniques. Molecular weights relative to polystyrene standards were determined by gel permeation chromatography (GPC) in THF and DMF as eluents with flow rates of 1 mL/min. The GPC instrument was equipped with three Polymer Labs columns (10^3 , 10^4 , and 10^5 Å) for THF as the eluent (40 °C) and four Water Ultrastaygel columns (500,

10^3 , 10^4 , and 10^5 Å) for DMF as the eluent (70 °C). The measurements were made by using UV and RI detectors, respectively.

A TA instrument 2910 differential scanning calorimeter was used to determine the thermal transitions. Indium was used as a standard for calibration. First-order transitions (e.g., mesophase-isotropic phase, etc.) were taken as the maximum or minimum of the endothermic or exothermic peaks. Glass transitions (T_g s) were taken as the half-height of the change in the heat capacity.

^1H and ^{13}C NMR spectra were recorded on a Varian XL-200 and XL-300 spectrometer, respectively. TMS was used as an internal standard.

Optical textures were studied with an Olympus polarizing optical microscope equipped with a Linkam hot stage and an Olympus photcamera.

X-ray powder and fiber diagrams of the polymer were recorded using Ni-filtered $\text{Cu K}\alpha$ radiation in a Statton camera. The X-ray camera length was calibrated with CaCO_3 .

Tensile tests were performed in an Instron Universal testing machine Model TTBM. The LCPUE was cast into a film between 0.1 and 0.2 mm thick and cut into ring samples 3.94 mm in width. The rings were elongated to break at a rate of 50 mm/min, at room temperature. These tests except for the sample thickness had been carried out in accordance with the specification of ASTM D412-87.

Results and Discussion

1. Constitution of the Segmented Polyurethane Elastomers. The reactivity of the isocyanate groups of 2,4- and 2,6-tolylene diisocyanate,¹⁴ by considering the combination of electronic and steric effects, gives the following sequence of reactivity: 4-NCO (2,4-TDI) > 2-NCO (2,6-TDI) > 2-NCO (2,4-TDI with 4-urethane) \geq 6-NCO (2,6-TDI with 2-urethane). Since equal reactivity of the hydroxyl end groups of PTMO, as well as of the Diol-6 end groups, can be assumed, which is not affected by the conversion of one of two hydroxyl groups into a

Scheme 2

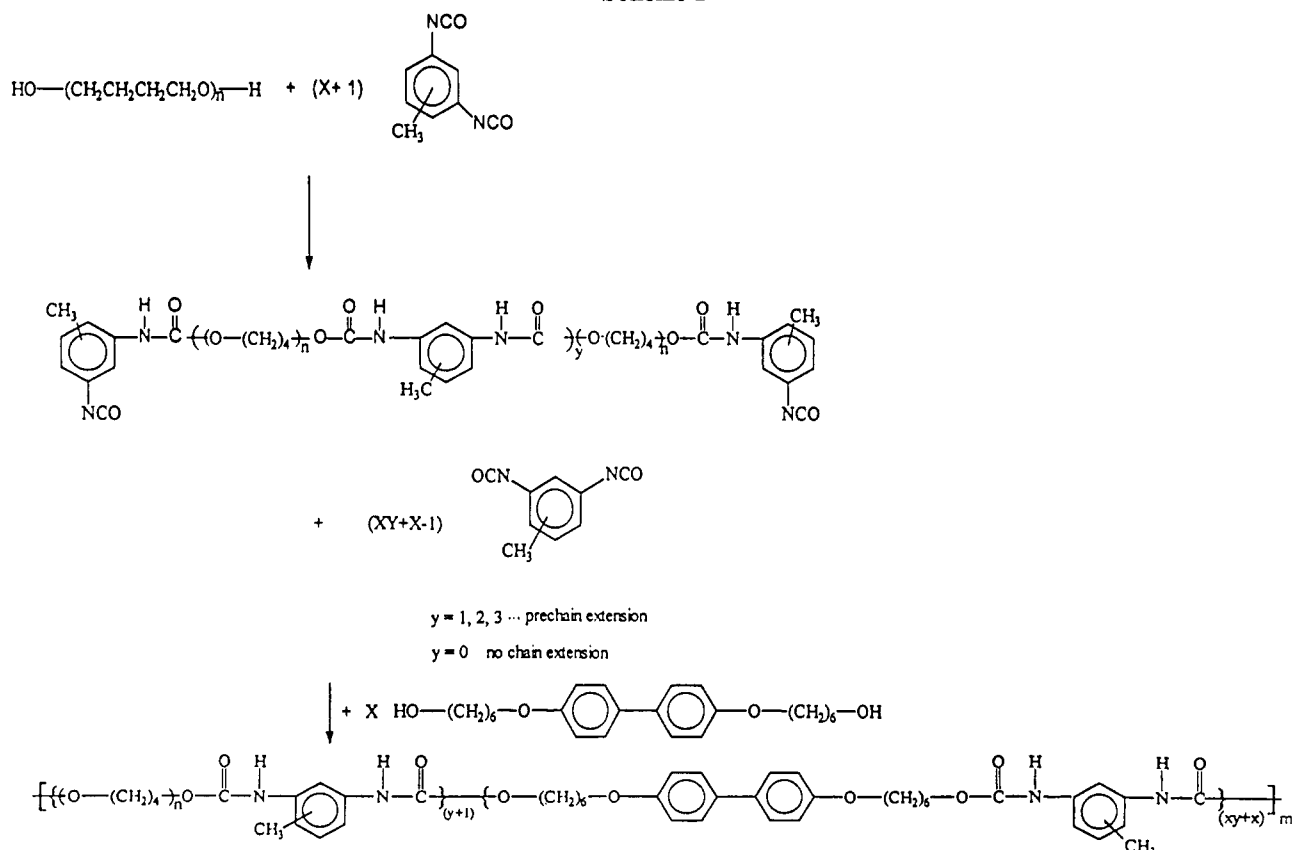


Table 1. Line Listing for ^{13}C NMR Resonances in Liquid-Crystalline Polyurethane Elastomers

region	range, ppm	specific key resonance, ppm	assignments	symbol
I	160–140	158.04	carbon bonded with oxygen in phenoxy	1
		154.25	carbonyl group of 2,6 urethane group	2
		153.7, 153.61	carbonyl group of 2,4 urethane group	2
II	140–100	136.72, 136.19, 136.08	carbon bonded with urethane group in phenyl group	3
		133.23	carbon between the biphenyl group	4
		130.66	carbon bonded with CH_3 in phenyl group	5
		127.57, 126.51	carbon bonded with hydrogen in biphenyl group	6
		114.61	carbon bonded with hydrogen in phenyl group	7
III	74–60	70.76–69.88	$-\text{CH}_2\text{O}-$ in PTMO	8
		67.70	CH_2 bonded with phenoxy in Diol-6	9
		65.26	CH_2 bonded with the urethane groups	13
IV	30–20	29.12, 28.81	CH_2 next to CH_2 (67.7 ppm chemical shift) in Diol-6	11
		26.10	$-\text{CH}_2-$ in PTMO and Diol-6	12
		25.74, 25.61	CH_2 next to CH_2 (65.26 ppm chemical shift) in PTMO and Diol-6	10
V	20–10	16.96	CH_3 of 2,4-TDI	14
		12.04	CH_3 of 2,6-TDI	15

Table 2. Molar Mass Characterization Obtained from GPC Analysis in THF and DMF Solvents

polymer	in THF solvent		in DMF solvent	
	M_w	MMD ^a	M_w	MMD
LCPUE 650	60 000	2.17	32 100	1.82
LCPUE 1000	75 400	2.00	42 500	1.95
LCPUE 2000	45 700	1.84	33 600	2.01

^a MMD = \bar{M}_w/\bar{M}_n .

urethane linkage, the difference of the reactivity of the isocyanate groups in the system has no specific effect on the 2,4- and 2,6-TDI distribution along the chain; i.e., the TDI isomers are randomly built into the chain.

The possible prechain extension of poly(tetramethylene oxide) with TDI during the prepolymer formation¹³ is shown in Scheme 2, and the relatively small amount of residual TDI reacts with Diol-6 in the following chain extension reaction to form longer hard segments. In this context, the polydispersity of the PTMO should also be discussed. The idealized hard-segment structure is perturbed by the incorporation of Diol-6 repeating units, and low molar mass homologues of the $\text{H}-[\text{O}(\text{CH}_2)_4]_n-\text{OH}$ series, especially with $n = 1, 2$, might not contribute to the soft segment of the segmented block copolymer but participate in the liquid crystalline hard domain formation.

Table 2 shows the average molar masses and molar mass distributions (MMD) of the polymers as obtained from GPC measurements in two different solvents. The MMD values are close to 2, expected for conventional condensation polymerization. The relative molar masses, compared with polystyrene standards, are comparable to those of conventional polyurethane elastomers. The difference in the molar masses obtained from THF and DMF as solvents (eluent) reflects the fact that THF is a poor solvent for the liquid crystalline hard segments and their possible aggregation in THF, especially evident for the LCPUE 650 sample. This illustrates the importance of the proper choice of a solvent as the eluent in molar mass determination.

2. Thermal Characterization.^{15,16} DSC thermograms for LCPU and LCPUE are shown in parts A and B of

Table 3. Thermal Properties of LCPUE by DSC

sample	soft segment $T_g/^\circ\text{C}$	hard segment		
		$T_{i(1)}/^\circ\text{C}^a$	$T_{i(2)}/^\circ\text{C}^b$	$\Delta H_i/(\text{mol}/\text{kJ})^c$
LCPUE 650	-25	103	126	12.0
LCPUE 1000	-51	101	128	9.9
LCPUE 2000	-73	105	121	5.1

^a Peak temperature of the low endotherm (Figure 1b). ^b Peak temperature of the high endotherm (Figure 1b). ^c Heat of isotropization of the sample annealed at 105 $^\circ\text{C}$ for 3 h (Figure 3).

Figure 1. In the low-temperature region, Figure 1A and Table 3 show a decrease and narrowing of the T_g of the soft segment of LCPUE with an increase of the soft-segment molar mass. The endotherm in Figure 1A represents melting of the soft-segment crystallites in LCPUE 2000. It has been suggested that the critical molar mass required for PTMO soft-segment crystallization in segmented polyurethanes is about 3000.¹⁷ In the present case, this is achieved by prechain extension during the prepolymer formation of LCPUE 2000.¹³

In the high-temperature region (Figure 1B), a distinct endothermic peak around 145 $^\circ\text{C}$ is found for LCPUE. High-temperature polarizing optical microscopy shows that this corresponds to the isotropization temperature (T_i). Compared with the LCPUE homopolymer, the endotherm in LCPUE is shifted to lower temperature and appears to consist of two endotherms separated by an exotherm. The lower temperature endotherm occurs at ca. 100 $^\circ\text{C}$, and the higher temperature endotherm occurs at ca. 128 $^\circ\text{C}$ (Table 3). High-temperature X-ray powder diffraction patterns show that the second endotherm is related to the mesophase–isotropic phase transition. The depression of T_i relative to that of LCPUE is associated with the oligomeric structure of the hard segment in the LCPUE. This is similar to the behavior of the melting points (T_m) of 2,4-TDI and 1,4-butanediol model oligomers with different numbers of repeating units and structural regularity.¹⁸ Monodisperse hard-segment polyurethane elastomer studies^{13,19,20} have also shown a decrease of the transition temperature with a decrease of the number of repeating units in the hard segment. Furthermore, the broadening

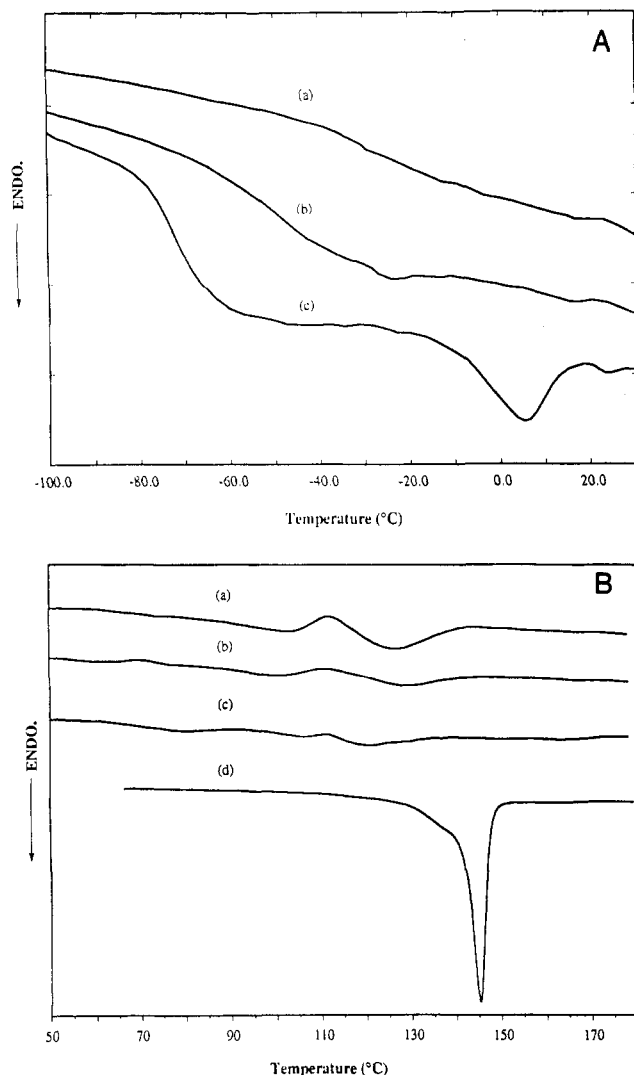


Figure 1. (A) DSC low-temperature thermograms for LCPUE at a heating rate of 10 K/min: (a) LCPUE 650, (b) LCPUE 1000, (c) LCPUE 2000. (B) DSC high-temperature thermograms for LCPUE at a heating rate of 10 K/min: (a) LCPUE 650, (b) LCPUE 1000, (c) LCPUE 2000, (d) LCPUE.

of the endotherm in the LCPUE reflects the lack of uniformity of the mesophase domains. It could be caused by structural irregularity in the mesophase resulting from the incorporation of butanediol and dihydroxydibutyl ether in the hard segments (Scheme 2, $n = 1, 2$ in PTMO) and/or by the distribution of micromesophase sizes and the influence of the structure of the interfacial region.

Figure 2 shows the DSC traces of LCPUE 650 at different heating rates. At the slow heating rate of 2 K/min (Figure 2, curve a), there is predominantly one broad endotherm at about 120 °C, corresponding to the high-temperature original endotherm. As the heating rates are increased, the low-temperature endotherm increases at the expense of the high-temperature endotherm. For the 80 K/min heating rate, the low-temperature endotherm predominates, and the high-temperature endotherm is only visible as a weak shoulder (Figure 2, curve d). This behavior can be explained by the existence of two mesophases of different thermodynamic stability in the LCPUE. The melting behavior of model compounds suggests it might be related to 2,4-TDI and Diol-6 isomeric structure. At sufficiently low heating rates, the thermodynamically more stable phase is created during heating by the reorganization of the less stable one. Similar thermal behavior has also been observed for LCPUE 1000 and 2000.

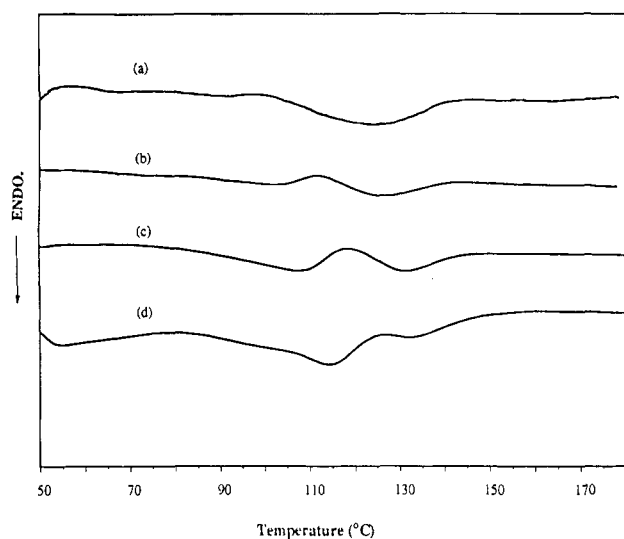


Figure 2. DSC thermograms for LCPUE 650 at different heating rates: (a) 2, (b) 10, (c) 40, (d) 80 K/min.

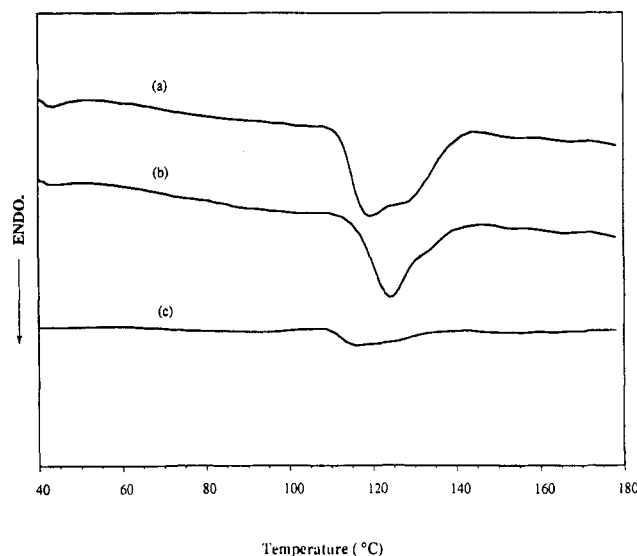


Figure 3. DSC thermograms for LCPUE at a heating rate of 10 K/min after annealing at 105 °C for 3 h: (a) LCPUE 650, (b) LCPUE 1000, (c) LCPUE 2000.

Annealing of LCPUE at 105 °C, which is above the isotropization temperature of the lower temperature mesophase, narrows the endothermic transition peak and yields the higher temperature mesophase (Figure 3). X-ray diffraction patterns of the annealed LCPUE samples show that the reflection at 4.5 Å sharpened substantially, indicating improved lateral packing order in the mesophase. Another interesting phenomenon is the increase of the heat of isotropization of the mesophase with decreasing soft-segment molar mass. This may be due to the contribution of the low molar mass fraction of poly-(tetramethylene oxide) in the formation of the mesophase. Especially in LCPUE 650, short oligo(tetramethylene oxide) chains can further extend the hard segments. The effect will decrease as the low molar mass fraction of poly-(tetramethylene oxide) decreases when the average molar mass increases.

Figure 4 shows that the development of the mesophase is both thermodynamically and kinetically controlled. If the LCPUE 650 sample quenched from the isotropic phase to 65 °C is heated immediately at a heating rate of 10 K/min (Figure 4, curve a), two distinct endotherms are observed separated by an exotherm. Following the same procedure, after quenching the sample to 75 °C, no endotherm appears in the subsequent heating cycle; but

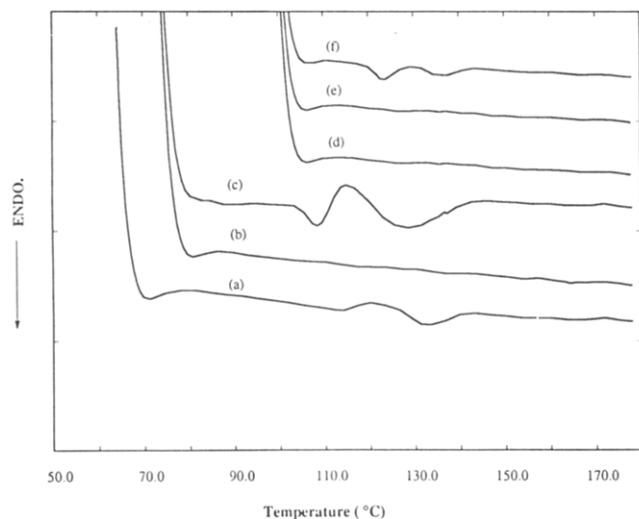


Figure 4. DSC thermograms for LCPUE 650 at a heating rate of 10 K/min after quenching the sample from 180 °C to the following temperature: (a) 65 °C, (b) 75 °C, (c) 75 °C and annealed at 75 °C for 20 min, (d) 100 °C, (e) 100 °C and annealed at 100 °C for 20 min, (f) 100 °C and annealed at 100 °C for 90 min.

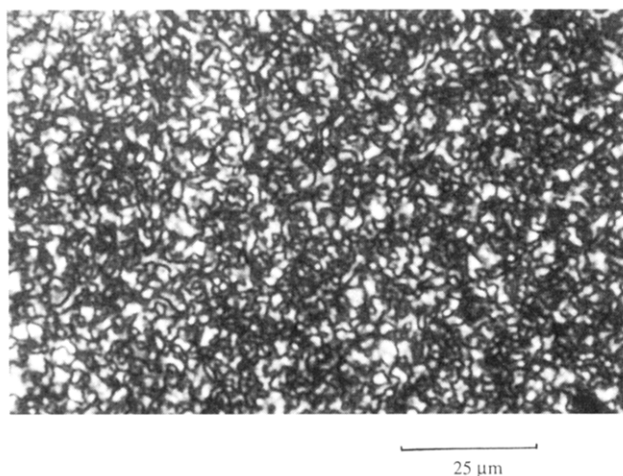


Figure 5. Polarizing optical micrograph of the LCPU mesophase obtained on cooling from the isotropic melt.

it is only upon annealing for, e.g., 20 min, that the endotherm appears again. Compared to this, a longer annealing time, e.g., 90 min, is required to observe the endothermic transition for the sample quenched to 100 °C. Curves a, b, and d in Figure 4 reflect the effect of thermodynamics on mesophase formation in the different supercooled samples. Comparison of curves b and c, as well as d or e and f, reveals the additional kinetic effects in mesophase formation. This systematic varying of the sample thermal history also indicates that the mesophase formation occurs from a liquid-liquid microphase-separated system.

3. Textural Observations with Polarizing Optical Microscopy. The observation of the LCPU sample which is cooled from the isotropic melt (155 °C) shows a Schlieren texture under the polarizing optical microscope (Figure 5). Unlike a nematic phase in which the Schlieren texture exhibits singularities with two brushes,²¹ this sample shows only singularities with four associated brushes. This suggests a smectic mesophase in the LCPU homopolymer.

For the LCPUE samples, no birefringence is observed under the polarizing optical microscope. This means that the size of the mesophase microdomain is smaller than the wavelength of the polarized light.

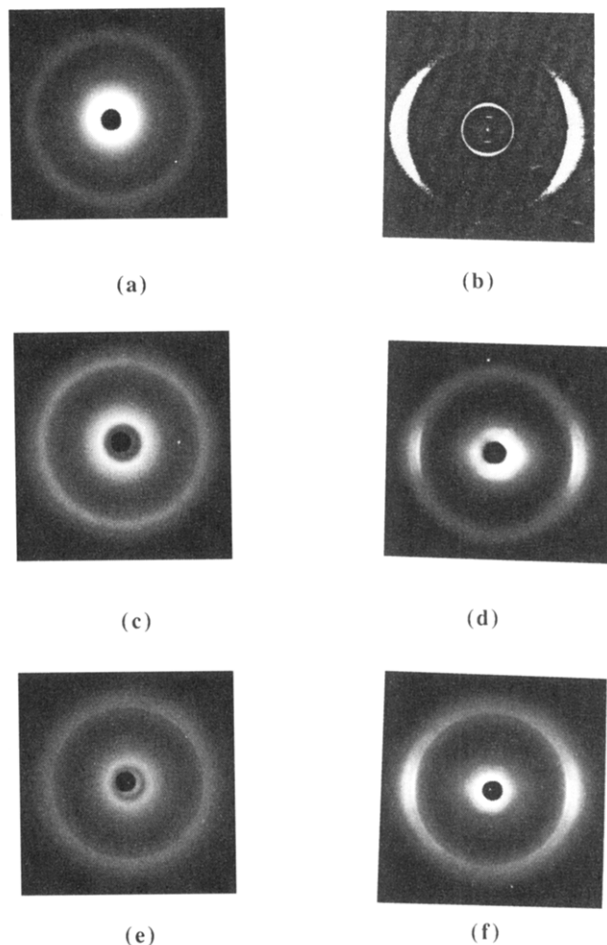


Figure 6. Room-temperature X-ray diffraction patterns: (a) LCPU sample without orientation; (b) LCPU fiber drawn from the melt; (c) unstretched LCPUE fiber drawn from the melt; (d) stretched LCPUE fiber drawn from the melt; (e) unstretched annealed LCPUE fiber; (f) stretched annealed LCPUE fiber.

4. X-ray Diffraction. X-ray diffraction patterns are presented in Figure 6 for the oriented and unoriented LCPU and LCPUE 1000 samples with different thermal histories.

Two distinct rings are observed in the unoriented LCPU sample (Figure 6a); a sharp inner one implies a lamellar spacing of 14.3 Å, which is indicative of long-range positional order in the structure. This is consistent with the layered morphology of a smectic phase. The diffuse outer ring occurring at 4.2–4.5 Å corresponds to the interchain spacing and reflects the packing of the molecules within the layers of the smectic phase.^{22,23}

Figure 6b shows the X-ray fiber pattern for the LCPU sample drawn rapidly from the melt. Instead of the outer ring in the unoriented sample, two diffuse equatorial arcs appear and correspond to an interchain spacing of 4.1–4.9 Å. Simultaneously, the intensity of the inner ring on the meridional position is increased, and additional reflections are present as well. Together with the Schlieren microscopic texture, these results indicate a smectic phase polydomain morphology.²⁴

Parts c and d of Figure 6 show the X-ray diffraction patterns for the unstretched and stretched LCPUE 1000 fiber drawn from the melt. The scattering from the liquid crystalline hard domain is superimposed on the scattering of the soft domain. One can discriminate the diffuse outer ring (4.3–4.6 Å) resulting from mesophase diffraction and the halo (3.8–4.7 Å) from the PTMO scattering. At 500% elongation, the increased equatorial arcs illustrate that

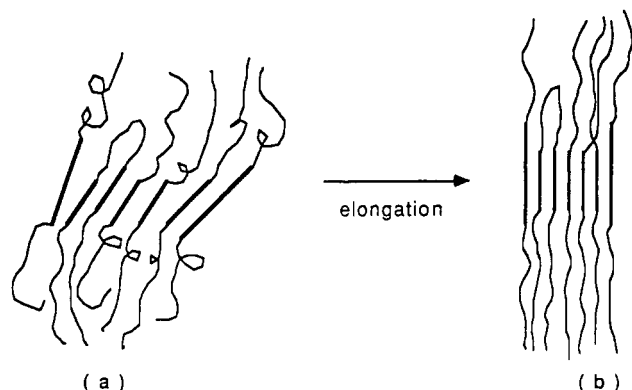


Figure 7. Schematic models for the aggregation of liquid crystalline hard segments in LCPUE: (a) unoriented sample, (b) oriented sample.

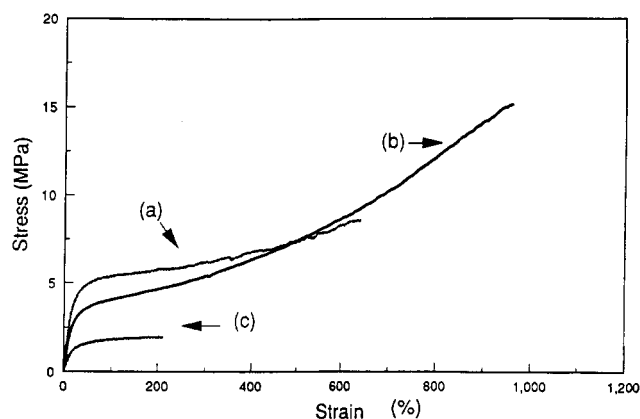


Figure 8. Stress-strain curves of LCPUE: (a) LCPUE 650, (b) LCPUE 1000, (c) LCPUE 2000.

the liquid crystalline domains are oriented uniaxially. The sharpening of the equatorial reflection at 4.5 Å, which is related to the spacing between the hard segments, suggests that there is an improvement of the lateral packing order in the mesophase. In this context, it has to be pointed out that such an improvement in chain packing can be achieved for multiblock copolymers with semicrystalline polyurethane hard domains only by a combination of stretching and annealing.^{25,26} This indicates the ease with which mesophase hard domains can be reorganized by stress, because of their flow properties. Figure 7 illustrates a schematic model for the improvement of the packing of the mesophase in a hard domain and its alignment upon elongation.

The effect of annealing on the X-ray diffraction pattern of LCPUE 1000 fiber drawn from the melt is shown in parts e and f of Figure 6. A total of 3 h of annealing at 105 °C improves the mesophase order, and a sharp reflection at 4.5 Å is observed. The agreement of the spacing observed with that of the biphenyl distance in a liquid crystalline polyurethane of 2,6-TDI and Diol-6⁶ suggests a similarity between the mesophase in the hard domains of the elastomer and the development of a lateral register between the neighboring biphenyl groups during the thermal treatment. As for the unannealed sample, Figure 6f illustrates that elongation leads to perfection and orientation of the mesophase.

5. Tensile Tests. The stress-strain properties of LCPUE are shown in Figure 8. It is obvious that the mesophasic hard-segment content has a profound effect upon the stress at a given strain probably due to a filler effect. Since the overall molecular weights of these samples are comparable, the distinct differences in elongation at break can be attributed to the morphological differences

in these LCPUE samples. As compared with LCPUE 1000 and 650, the relatively small content of the mesophase in LCPUE 2000 leads to low tensile properties and elongation at break. The superior tensile properties of LCPUE 1000 and 650 may result from the presence of a lamellar or possibly bicontinuous mesophase and an amorphous soft phase.²⁷

Conclusion

In this type of main-chain liquid crystalline elastomer, the formation of a mesophase is achieved by the self-assembly of the hard segments. The elastic deformation can orient the mesophase and lead to macroscopic anisotropy in the material. The elasticity results from the conformational entropy change of soft segments.

Acknowledgment. We are grateful to the Army Research Office (Grant DAAL03-91-G-0127) for financial support of this research, and the use of Central Facilities of Materials Research Laboratory (MRL) is also gratefully acknowledged.

References and Notes

- Finkelmann, H.; Kock, H. J.; Rehage, G. *Makromol. Chem., Rapid Commun.* **1981**, *2*, 317.
- Schätzle, J.; Kaufhold, W.; Finkelmann, H. *Makromol. Chem.* **1989**, *190*, 3269.
- Mormann, W.; Benadda, S. *Polym. Prepr. (Am. Chem. Soc., Div. Polym. Chem.)* **1993**, *34* (2), 739.
- Lorenz, R.; Els, M.; Haulena, F.; Schmitz, A.; Lorenz, O. *Angew. Makromol. Chem.* **1990**, *180*, 51.
- Stenhouse, P. J.; Valles, E. M.; Kantor, S. W.; MacKnight, W. J. *Macromolecules* **1989**, *22*, 1467.
- Papadimitrakopoulos, F.; Hsu, S. L.; MacKnight, W. J. *Macromolecules* **1992**, *25*, 4671.
- Iimura, K.; Koiede, N.; Tanabe, H.; Takeda, M. *Makromol. Chem.* **1981**, *182*, 2569.
- Mormann, W.; Brahm, M. *Macromolecules* **1991**, *24*, 1096.
- Tanaka, M.; Nakaya, T. *J. Macromol. Sci. Chem.* **1987**, *A24* (7), 777.
- Stenhouse, P. J. Ph.D. Thesis, University of Massachusetts at Amherst, Amherst, MA.
- Sandler, S. R.; Karo, W. *Polymer Syntheses I*; Academic Press: New York, 1974; Vol. I, Chapter 8.
- Odian, G. *Principles of Polymerization*, 2nd ed.; John Wiley & Sons: New York, 1981.
- Eisenbach, C. D.; Baumgartner, M.; Gunter, C. *Advances in Elastomers and Rubber Elasticity*; Lai, J., Mark, J. E., Eds.; Plenum: New York, 1986; p 51.
- Ferstanding, L. L.; Scherrer, R. A. *J. Am. Chem. Soc.* **1959**, *81*, 4838.
- Copper, W.; Pearson, R. W.; Parke, S. *Ind. Chem.* **1960**, *36*, 121.
- Seymour, R. W.; Cooper, S. L. *Macromolecules* **1973**, *6* (1), 48.
- Miller, J. A.; Lin, S. B.; Hwang, K. S.; Wu, K. S.; Gibson, P. E.; Cooper, S. L. *Macromolecules* **1985**, *18*, 32.
- Cheng, S. Z. D. *Macromolecules* **1988**, *21*, 2475.
- Seefried, C. G.; Koleske, J. V.; Critchfield, F. E. *J. Appl. Polym. Sci.* **1975**, *19*, 2493.
- Fu, B.; Feger, C.; MacKnight, W. J.; Schneider, N. S. *Polymer* **1985**, *26*, 889.
- Harrell, L. L., Jr. *Macromolecules* **1969**, *2* (2), 607.
- Eisenbach, C. D.; Neffzger, H. *Multiphase Macromolecular Systems*; Culbertson, B. M., Eds.; Plenum: New York, 1989; p 339.
- Gray, G. W.; Goodby, J. W. G. *Smectic Liquid Crystals*; Leonard Hill: 1984.
- Azaroff, L. V. *Mol. Cryst. Liq. Cryst.* **1987**, *145*, 31.
- De Vries, A. *Mol. Cryst. Liq. Cryst.* **1985**, *131*, 125.
- Azaroff, L. V. *Mol. Cryst. Liq. Cryst.* **1980**, *60*, 73.
- Falgouttes, J.; Delord, P. *Liquid Crystals and Plastic Crystals*; Gray, G. W., Winsor, P. A., Harwood: Sussex, U.K., 1974; Vol. 3, p 62.
- Blackwell, J.; Lee, C. D. *J. Polym. Sci., Polym. Phys. Ed.* **1983**, *21*, 2169.
- Blackwell, J.; Lee, C. D. *J. Polym. Sci., Polym. Phys. Ed.* **1984**, *22*, 759.
- Thomas, E. L.; Reffner, J. R.; Bellare, J. International Workshop on Geometry and Interface, Sept 1990, C7-363.